

Study on IR Properties of Reduced Graphene Oxide

Deyue Ma¹, Xiaoxia Li^{1,2}, Yuxiang Guo^{1,2} and Yurun Zeng¹

¹State Key Laboratory of Pulsed Power Laser Technology, Hefei 230037, China

²Key Laboratory of Infrared and Low Temperature Plasma of Anhui Province, Hefei 230037, China

*Corresponding author e-mail: madeyuexs@163.com

Abstract. Firstly, the reduced graphene oxide was prepared by modified hummer method and characterized. Then, the complex refractive index of reduced graphene oxide in IR band was tested and its IR absorption and radiation properties were researched by correlated calculation. The results show that reduced graphene oxide prepared by hummer method are multilayered graphene with defects and functional groups on its surface. Its absorption in near and far IR bands is strong, but it's weaker in middle IR band. At the IR atmosphere Window, its normal spectral emissivity decreases with wavelength increasing, and its total normal spectral emissivity in 3 ~ 5 μ m and 8 ~ 14 μ m are 0.75 and 0.625, respectively. Therefore, reduced graphene oxide can be used as IR absorption and coating materials and have a great potential in microwave and infrared compatible materials.

1. Introduction

Graphene is a two-dimensional crystal material formed by infinite expansion of the sp^2 hybrid carbon atom benzene ring unit [1]. This two-dimensional lattice structure makes it have excellent mechanical, thermal, electrical and optical properties. Monolithic graphene has only 2.3% of absorption in optical band, 5300W/(m \cdot K) of thermal conductivity, 15000cm²/(V \cdot s) of electron mobility at room temperature, and only about 10⁻⁶ $\Omega\cdot$ cm of resistivity [2]. These excellent properties make it have broad application prospects in the electronic device [3], sensor [4], transparent conductive material [5], composite material [6], energy storage material [7], absorbing materials [8], and so on.

Because of its excellent electromagnetic properties, the reduced graphite oxide(RGO) has been widely used as microwave absorbing material [9]. Meanwhile, although the ideal graphene has weak absorption in IR band, the IR absorption of RGO prepared by hummer method may be enhanced by the presence of defects and functional groups. Therefore, RGO has a great application potential in microwave and infrared compatible materials. In this paper, the RGO is prepared by hummer method and characterized, and then its IR absorption and emission performance is analyzed, which provides a good foundation for the application of RGO in microwave and IR compatible materials.



2. Experiment and Instruments

2.1. Preparation

The preparation method of RGO was modified hummer method and its process was as follows: 2g of natural graphite (80 mesh, purity 99.9%) was mixed with 200ml of acid mixture which contain H_2SO_4 (Concentration 99%, AR) and H_3PO_4 (concentration 85%, AR) with a volume ratio of 9: 1 in a three-necked flask. Then 1g of potassium permanganate (purity 99.5%, AR) was added in several times, and stirred for 1h in ice bath. The reaction was carried out for 10h at 70°C. The hydrogen peroxide (concentration 30%, AR) was added to the product, until the solution color became golden yellow. After filtration, the product was washed until its pH close to 7. Here, graphite oxide was obtained.

Graphite oxide was dispersed in deionized water by sonication for 2 h. Then, 0.6 g KOH (purity 99.5%, AR) and 4 mL hydrazine hydrate (concentration 80%, AR) were added to the suspension and reacted at 100 °C for 24 h. After cooling down, the product was washed and dried to obtain RGO.

2.2. Instruments

Using the SE900-50 IR spectrum ellipsometry (Band range: 650~4000 cm^{-1}) from Sentech company to measure complex refractive index. The emissivity was obtained by IR-dual-band emissivity measuring instrument from Shanghai Technical Physics Institute. Using Nicolet 8700 IR spectrometer (Band range: 400~4000 cm^{-1}) to analyze the IR transmission spectra of RGO. Raman spectroscopy was performed by RENISHAW in Via laser confocal Raman spectrometer (wavelength: 532nm, spectral range: 200~1000nm, spectral resolution: 1 cm^{-1}).

3. Results and Analysis

3.1. Characterization analysis

The results of IR spectroscopy and Raman scattering spectra are shown in Figure 1 and Figure 2.

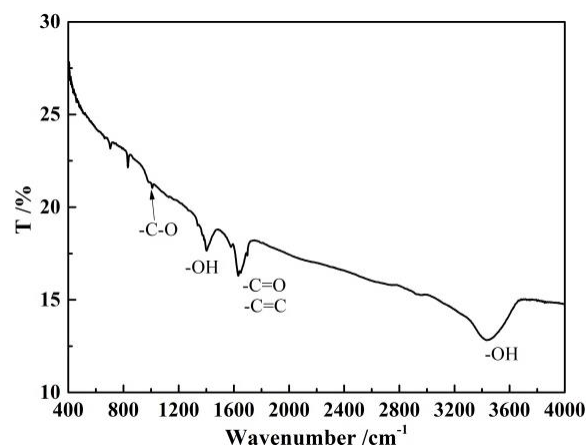


Figure 1. The IR spectrum of reduced graphene oxide

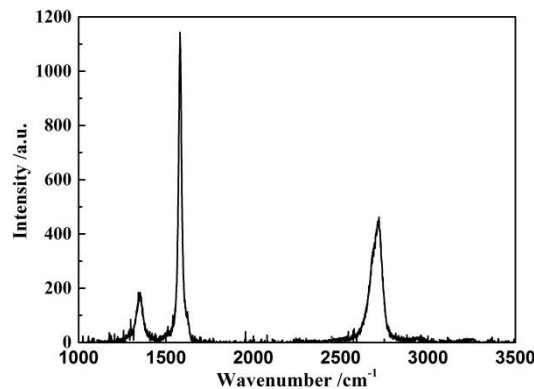


Figure 2. The Raman spectrum of reduced graphene oxide

Figure 1 shows that RGO has some absorption peaks owing to -C=O stretching vibration (1720 cm^{-1}), C=C stretching vibration (1640 cm^{-1}), -OH deformation (1390 cm^{-1} , 3450 cm^{-1}), -C-O stretching vibration (1002 cm^{-1}) [10]. There is no obvious absorption peak of ideal graphene in the IR spectrum, which indicates that there are still functional groups such as -OH , -COOH , -C-O and -C=O on RGO.

It can be seen from Figure 2 that RGO has D peak at 1342 cm^{-1} with strength of 186, G peak at 1594 cm^{-1} with strength of 1143, and 2D peak at 2720 cm^{-1} with strength of 461. The intensity ratio of the D and G peak (I_D/I_G) is generally used to characterize defect density on RGO which is proportional to I_D/I_G . I_D/I_G of the ideal graphene is 0.06 [11], and it's 0.16 to RGO which means a relatively low defect density. The higher the intensity ratio of 2D and G peak (I_{2D}/I_G), the fewer the number of layers to RGO. The I_{2D}/I_G of single layer graphene is generally above 2^[12], and to RGO it's 0.4, so RGO prepared by modified hummer method is multilayered.

3.2. Analysis of Its IR Band Performance

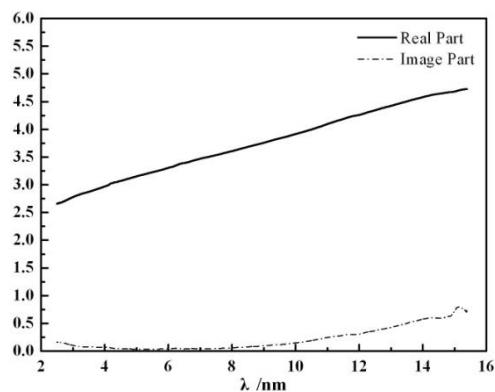


Figure 3. The complex refractive index of RGO in IR band

At room temperature, complex refractive index of RGO in IR band was measured by ellipsometry. The results are shown in Figure 3.

It can be seen from Figure 3 that the real part of complex refractive index is more than 2.6. But the imaginary part in middle IR band is almost 0, and only in the far-IR band it's relatively larger. The absorption coefficient $\alpha(\lambda)$ of RGO can be expressed by formula (1) [13], and the calculation results are shown in Figure 4.

$$\alpha(\lambda) = \frac{2k}{\lambda n} \quad (1)$$

Where λ is wavelength, k is the imaginary part of complex refractive index, and c is the speed of light.

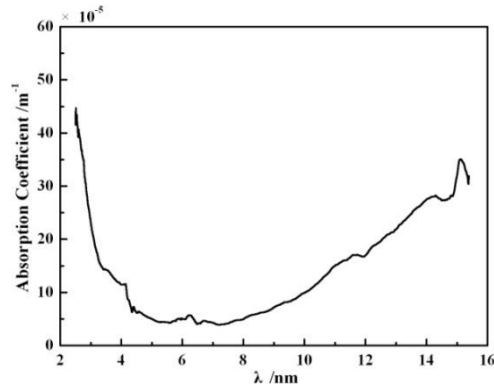


Figure 4. The absorption coefficient of RGO

Figure 4 shows that the absorption coefficient of RGO in 10~15.8 μm and 2.5~4 μm is in order of 10^{-4} , and the absorption coefficient is very small in 4~10 μm , only in order of 10^{-5} , which means weak absorption. According to the theory of atomic cluster absorption, the size and absorption peak wavelength λ_a of atomic clusters can be expressed by (2) [14]:

$$\lambda_a = L \cdot \sqrt[3]{N} \cdot 1.674 \cdot 10^3 \quad (2)$$

Where L is the size of the cluster, N is the number of π electrons in cluster, and the calculation method of N is given in reference [14].

RGO can be regarded as carbon clusters with several nanometers thick which has absorption peak in 2~4 μm , and the hydroxyl group on RGO belongs to near IR absorption group. The absorption band range of lattice vibration is 5~15 μm . However, the defects and functional groups on it break its original lattice structure, exacerbate the lattice vibration, and enhance its absorption performance in 10~15.8 μm . That's why RGO has better absorption performance in these bands.

For the solids with a smooth surface and opaque in the measuring band, the normal emissivity ε can be calculated by formula (3) [15]:

$$\varepsilon = 1 - \frac{(n_2 \cos \theta_{in} - n_1 \cos \theta_t)^2 + (k_2 \cos \theta_t - k_1 \cos \theta_{in})^2}{(n_2 \cos \theta_{in} + n_1 \cos \theta_t)^2 + (k_2 \cos \theta_t + k_1 \cos \theta_{in})^2} \quad (3)$$

Where θ_m is the incidence angle; θ_t is the refraction angle; n_1 and k_1 are real and imaginary parts of complex refractive index to the incident medium; n_2 and k_2 are real and imaginary parts of complex refractive index to the refraction medium.

Due to its complex refractive index, the refraction angle should be calculated by formula (4)^[16]:

$$\sin \theta_t = \frac{n_1 \sin \theta_{in}}{\sqrt{\frac{1}{2} \left[(n_2^2 - k_2^2 - n_1^2 \sin^2 \theta_{in})^2 + 4n_2^2 k_2^2 + (n_2^2 - k_2^2) + n_1^2 \sin^2 \theta_{in} \right]}} \quad (4)$$

Using the measured results, RGO normal spectral emissivity is calculated from equations (3) and (4). At the IR atmospheric window (3~5 μm , 8~14 μm), complex refractive index of air can be considered as 1, which is $n_1 = 1$ and $k_1 = 0$, and the calculated results are shown in Figure 5.

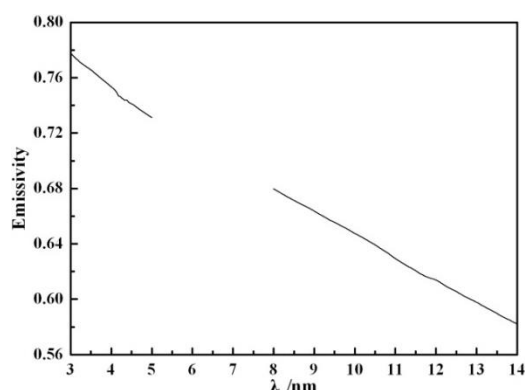


Figure 5. The normal spectral emissivity of RGO

It can be seen from Figure 5 that the normal emissivity of RGO at 3~5 μm is in range of 0.73 ~ 0.778 and decreases with the increase of wavelength. At 8 ~ 14 μm , the normal emissivity decreased from 0.679 to 0.583 with wavelength increasing too. To verify the accuracy of the calculated results, the total emissivity of the two bands were measured and the results are 0.75 and 0.625, respectively. Then, they were calculated by combining the Planck formula and Steven Boltzmann's law with the measured spectral emissivity. The calculated results are 0.7427 and 0.6323, which means the error between the measured and calculated results are very small. Therefore, the calculated normal spectral emissivity can be a good reflection of RGO radiation properties at IR atmospheric window.

4. Conclusion

In this paper, RGO was prepared by modified hummer method. From the characterization analysis and measured results, we can see that RGO are multilayered with functional groups and defects on surface which make RGO has a strong absorption in 2.5~4 μm and 10~15.8 μm . Simultaneously, its spectral emissivity decreases with the increase of wavelength at IR atmospheric window, and the total emissivity at 3~5 μm and 8~14 μm are 0.75 and 0.625 respectively which are identical with the test results. Therefore, RGO can be used as IR absorption and coating materials, and has a great potential in using as microwave and IR compatible materials.

Acknowledgments

This work was financially supported by national youth science fund (No.61405248).

References

- [1] J.C. Meyer, A.K. Geim, M.I. Katsnelson, et al, The structure of suspended graphene sheets, *Nature* 446 (7131) 60-66.
- [2] L. Liu, M. Qing, Y. Wang, et al, Defects in graphene: generation, healing, and their effects on the properties of graphene: a review, *J. Mater. Sci. Technol.* 31 (6) 599-606.
- [3] S.J. Li, S. Gan, H.R. Mu, et al, Research progress in graphene use in photonic and optoelectronic devices, *New. Carbon. Mater.* 29 (5) 329-356.
- [4] K. Dhara, J. Stanley, T. Ramachandran, et al, Pt-CuO nanoparticles decorated reduced graphene oxide for the fabrication of highly sensitive non-enzymatic disposable glucose sensor, *Sensor. Actuat. B-Chem* 764 (195) 197-205.
- [5] S. Eigler. A new parameter based on graphene for characterizing transparent, conductive materials, *Carbon* 47 (12) 2936-2939.
- [6] X.Y. Wu, S.M. Li, J.H. Liu, et al. Preparation and microwave absorption properties of CoFe_2O_4 -graphene nanocomposites, *J. Inorg. Mater.* 29 (8) 845-850.
- [7] H.T. Zhang, H. Hu, B. Gu, et al, Preparation and properties of polyvinylidene fluoride-zeolite composite lithium diaphragm, *Acta. Mater. Compos. Sin.* 33 (10) 1-7.
- [8] B. Yao, C.G. Cheng, M. Li, et al, Advanced in innovative nanometer carbon-based

- electromagnetic wave absorbing composites, *Materials Review* 30 (19) 77-83.
- [9] C. Wang, X. Han, P. Xu, et al, the electromagnetic property of chemically reduced graphene oxide and its application as microwave absorbing material, *Appl. Phys. Lett.* 98 (7) 217-223.
- [10] T. Szabó, E. Tombácz, E. Illés, et al, Enhanced acidity and pH-dependent surface charge characterization of successively oxidized graphite oxides, *Carbon* 44 (3) 537-545.
- [11] A.C. Ferrari. Raman Spectroscopy of graphene and graphite: disorder, electron-phonon coupling, doping and nonadiabatic effects, *Solid State Commun.* 143 (1-2) 47-57.
- [12] J.Y. Long, T. Huang, X.H. Ye, et al, Effects of low power CO₂ laser irradiation on structure of multilayer grapheme, *Ch. J. Las.* 2012 (12) 131-135.
- [13] J.P. Fan, H.M. Liu, Q. Tian, The imaginary part of dielectric function and the absorption coefficient, *Coll. Phys.* 28 (3) 24-25.
- [14] Q.Q. Gou, Electronic energy levels and absorption spectra of metal clusters and carbon clusters, *J. Atom. Mol. Phys.* 11 (4) 337-347.
- [15] B.A. Xiao, L.H. Gong, R. Zeng, Analysis and simulation of metallic infrared emissivity, *Infrared Tech.* 30 (6) 358-360.
- [16] S.A. Kovalenko. Descartes-Snell law of refraction with absorption, *Semicond. Phys.* 4 (3) 214-218.